Clinical Radiology 74 (2019) 652.e11–652.e19

Contents lists available at ScienceDirect

Clinical Radiology

journal homepage: www.clinicalradiologyonline.net

# Papilloedema: diffusion-weighted imaging of optic nerve head

N. Ray [a], S. Vyas [a,*], N. Khandelwal [a], R. Bansal [b], V. Lal [c]

[a] *Department of Radiodiagnosis and Imaging, Post Graduate Institute of Medical Education and Research (PGIMER), Chandigarh, India*

[b] *Department of Ophthalmology, Post Graduate Institute of Medical Education and Research (PGIMER), Chandigarh, India*

[c] *Department of Neurology, Post Graduate Institute of Medical Education and Research (PGIMER), Chandigarh, India*

ARTICLE INFORMATION

*Article history:*
Received 12 November 2018
Accepted 2 May 2019

AIM: To establish the correlation between clinical grading of papilloedema and diffusion abnormalities of optic nerve head (ONH) on diffusion-weighted imaging (DWI).

MATERIALS AND METHODS: Brain magnetic resonance imaging (MRI), including readout segmented echo planar imaging-based DWI, was performed in 32 patients with papilloedema and the same number of age- and sex-matched controls. Clinical grading of papilloedema was done according to the modified Frisén scale. Two neuroradiologists independently evaluated the MRI for ONH hyperintensity and apparent diffusion coefficient (ADC) value of ONH. The comparison between papilloedema clinical grade and qualitative grade of ONH hyperintensity and its presence between cases and control groups were done using the Chi-square test and Fisher's exact test, respectively. The comparison between mean ADC value of ONH among different grades and between cases and controls were done using analysis of variance (ANOVA)-F-test and Student's *t*-test, respectively. Receiver operating characteristic (ROC) analysis was done to calculate a cut-off ADC value between the case and control groups.

RESULTS: Significant correlation between ONH hyperintensity and mean ADC value of ONH with clinical grades of papilloedema and between cases and control groups were found. ONH hyperintensity was found to be a highly sensitive (87.5% for both) and specific (specificity 97.1% and 98.6% for two observers) sign of papilloedema. A mean cut-off ONH ADC value was found to have high sensitivity (96.83%) and specificity (95.31%) to distinguish between the cases and controls.

CONCLUSIONS: Diffusion parameters of ONH have significant correlation with clinical grading of papilloedema and can serve as a surrogate marker for intracranial pressure.



## Introduction

Papilloedema is defined as optic disc swelling occurring secondary to raised intracranial pressure (ICP).[1] It has been suggested that raised ICP is transmitted along the subarachnoid space along the optic nerve (ON) resulting in

* Guarantor and correspondent: S. Vyas, Department of Radiodiagnosis & Imaging, PGIMER, Chandigarh, Chandigarh, 160012, India. Tel.: +91 8872016105.

*E-mail address:* sameer574@yahoo.co.in (S. Vyas).

https://doi.org/10.1016/j.crad.2019.05.005
0009-9260/

interruption of the metabolic processes leading to oedema, ischaemia and eventual visual impairment or loss.[2] Identifying papilloedema is of paramount importance as it not only serves as a tool to diagnose raised ICP, but can be used to assess the severity of the disease as well as therapeutic response.

Magnetic resonance imaging (MRI) is a non-invasive tool to assess the globe, ON, optic tract and the brain for associated pathologies leading to raised ICP.[3] Multiple MRI signs have been described in the setting of raised ICP of which optic nerve sheath (ONS) enlargement, ON tortuosity, flattening of posterior sclera, intraocular protrusion of ON papilla and partially empty sella were found in relatively more patients and are useful in the diagnosis of raised ICP[2]; however, Padhye *et al.*[4] found no significant correlation between the clinical parameters and MRI findings of papilloedema in patients with idiopathic intracranial hypertension (IIH).

Diffusion-weighted imaging (DWI) is an MRI technique based on the movement of water molecules in the tissue spaces.[5,6] Viets *et al.*[7] showed that ONH hyperintensity seen on DWI can be a potential sign of papilloedema on imaging with a specificity of 100%; however, the sensitivity of the sign is low suggesting that the absence of this sign does not rule out papilloedema. In a subsequent study by Salvay *et al.*,[8] significant correlation was found between the clinical grade of papilloedema and hyperintensity of ONH on DWI in patients with IIH. Both the studies were retrospective studies and did not consider and/or compare clinical grade with apparent diffusion coefficient (ADC) value of ONH, which is a quantitative measure of diffusion.

Moreover, obtaining good-quality DWI for the orbits by routine single-shot echo-planar imaging (ss-EPI) is challenging because of susceptibility and blurring artefacts.[9] The present study used a newer technique of DWI based on readout-segmented, multi-shot EPI sequences (rs-EPI) combined with parallel imaging as proposed first by Porter and Heidemann.[10] Various studies have found rs-EPI based DWI to be better than that based on ss-EPI in terms of image quality while evaluating the brain, skull base and paranasal sinus lesions.[11–16]

The purpose of this study was to look for correlation between the clinical grade of papilloedema according to the modified Frisén scale[17,18] and qualitative grading of ONH hyperintensity as well as with mean ADC value of ONH in patients with papilloedema. The aim of the study was to evaluate the potential of diffusion abnormalities of ONH as a surrogate marker of raised ICP.

## Materials and method

### *Cases and controls*

This was a single institution prospective study approved by the Institutional Ethics Committee. Ethical approval was obtained for both case and control groups. A total of 32 newly diagnosed patients with papilloedema (12 men, 20 women; mean age of 31.5 years and age range 23–58 years) were included in the study. Written informed consent was obtained from all patients prior to inclusion in the study. A total of 32 age- and sex-matched patients (12 men, 20 women; mean age of 30.5 years, age range 21–59 years) undergoing MRI for spine or musculoskeletal parts were taken as controls. Control group patients found to have any structural abnormality on MRI brain were excluded from the study. The control group patients were informed about the additional brain MRI sequences to be done and written informed consent was obtained from all the control participants as well. Patients with contraindications to MRI were excluded from the study. Patients with contraindications to gadolinium-based MRI contrast medium underwent only unenhanced MRI. Patients with significant comorbid or debilitating conditions that made sitting difficult did not undergo fundus photography as part of their clinical evaluation and underwent clinical grading and MRI only.

### *Clinical evaluation*

Patients visiting the neurology and/or ophthalmology clinic who were found to have papilloedema on fundus examination were further evaluated for best corrected visual acuity measured by Snellen's chart, intraocular pressure, and slit-lamp examination before and after pupillary dilatation (done by instilling tropicamide 0.8% and phenylephrine 5% eye drops). Fundus photography was done by digital colour fundus photography on Visupac 450 Plus camera (Carl Zeiss, Jena, Germany) for 25 patients. The remaining seven patients only underwent clinical fundus examination as fundus photography was not possible due to significant comorbidities. Grading of papilloedema was done by an experienced neuro-ophthalmologist according to the modified Frisén scale (grade 0, normal; grade I, blurring in nasal disc margin; grade II, blurring of temporal disc margin without vessel obscuration; grade III, one or more segments of major vessel obscuration while crossing the optic disc without obscuration at the origin; grade IV, total obscuration of a major artery or vein at its central origin; and grade V, obscuration of all vessels both on the disc and leaving the disc).[17,18] The patients in the control groups were subjected to only clinical fundus examination to rule out the presence of papilloedema.

### *MRI evaluation*

All the patients in the case group underwent MRI examination on the same day as clinical examination to achieve maximum clinicoradiological correlation. MRI examinations were performed for all patients on a 1.5 T MRI system (Magnetom Aera system; Siemens Healthcare, Erlangen, Germany) using a dedicated 16-element head coil. The patients were asked to close their eyes gently and try not to move the eyeball as far as practicable to reduce motion artefacts during the scanning period. The MRI sequences those were used after a three-plane initial localiser sequence include axial T2 and fluid attenuated inversion recovery (FLAIR) imaging for brain, pre- and post-contrast

T1-weighted (W) three-dimensional (3D) ultrafast gradient echo (MPRAGE) for brain imaging, 3D fast imaging employing steady state precession (CISS) at the level of orbits, coronal T2 fat-saturated image of the orbit and time of flight (TOF) MRI venogram. Contrast-enhanced MPRAGE sequence was not done in two patients who had a history of allergy to gadolinium-based contrast agents. DWI of the brain was done using dedicated software (SYNGO RESOLVE), acquiring DWI by readout-segmented, multi-shot EPI sequence [rs-EPI] coupled with generalised auto-calibrating partially parallel acquisitions (GRAPPA). The sequence was acquired in an axial two-dimensional plane with repetition time (TR)=7,400 ms, echo time (TE)=74 ms, on a 224×224 matrix and field of view (FOV) of 230×100 mm (read-×phase) with b-values of 50 s/mm$^2$ and 1,000 s/mm$^2$. The section thickness used was 2 mm with an intersection gap of 0.4 mm and distance factor of 20%. The total number of sections and number of readouts were 33 and 7, respectively. Duration for the acquisition of the DWI sequence was 6 minutes 34 seconds. The control group of the patients were subjected to the same protocol except for the sequences CISS, coronal T2 sequence of orbit and TOF MR venography as these sequences were unnecessary given their clinical situation.

All the MRI images were evaluated by two neuroradiologists who had 10 years and 5 years of experience of evaluating MRI brain, respectively. Both the observers were blinded to the clinical grading of the patients' disease. The signal intensity (SI) of the each ONH on DWI at b=1,000 s/mm$^2$ was assessed and graded as normal, mild, or marked by both the observers. ONH SI was considered normal if equal to or less than that of the globe margin, mild if only slightly higher than that of the sclera, and marked if distinctly higher compared to the globe margin.

The system-generated ADC maps were evaluated by both the observers and the ADC value of ONH was calculated by both the readers independently. A circular or elliptical region of interest (ROI) was placed at the area of hypointensity at ONH corresponding to the area of hyperintensity in the b=1,000 images. In case the hyperintensity at ONH was not seen on DWI isotropic trace images at b=1,000, the ROI was placed arbitrarily at the ONH covering at least half to two-thirds of the ONH in the b=50 images and transferred to the ADC map. Generally, the average area of the ROI was 3–7 mm$^2$ and on an average 2–4 pixels were covered in the ROI. The ADC values were calculated at consecutive sections depicting the ONH and mean ADC value of those obtained in the section was calculated. At least two sections were included for all cases. Generally, one or more attempts (range 1–3) were required for placement of the ROI by the observers on ADC map; however, the best possible ROI was chosen according to the observer's discretion. The average time required for placement varies between 30 seconds to 2 minutes. Both the observers tried to avoid areas with cerebrospinal fluid (CSF) or vitreous signal intensity within the ROI. Appropriate zooming of the ADC maps was done for proper placement of ROI when required. In control participants, the DWI isotropic trace images at b=1,000 s/mm$^2$ and ADC maps were evaluated using the same principle of calculation of ADC value used for the case group.

### *Statistical analysis*

The statistical analysis was done using SPSS software version 17 (Statistical Packages for the Social Sciences, Chicago, IL, USA). A $p$-value of $<0.05$ was considered to indicate statistical significance. The following comparisons were made for each reader: (1) chi-square test for association between modified Frisén scale and ONH hyperintensity, (2) Fisher's exact test for comparison between cases and controls for the presence of ONH hyperintensity, (3) analysis of variance (ANOVA)-F (analysis of variance) test for comparison between papilloedema and mean ADC values of ONH in different clinical grades of papilloedema, and (4) Student's $t$-test for comparison between ADC value of ONH in cases and controls. In addition, receiver operating characteristic (ROC) analysis was performed for the ADC values calculated by two observers for each ONH in case and control participants as well as for the mean of ADC values calculated by both the observers. The normality of distribution of ADC value by each observer and mean ADC value in case and control groups was checked by the Shapiro–Wilk test. The interobserver agreement was calculated using kappa statistics for the ONH hyperintensity and by Bland–Altmann plot analysis for ADC value measurement.

## Results

All 32 patients were found to have bilateral papilloedema making the total number of eyes ($n$) to be 64. Twenty had IIH, while four each had intracranial tumours and meningitis, three had cerebral venous sinus thrombosis, and one had drug-induced raised ICP (acute promyelocytic leukaemia patient receiving all-trans-retinoic acid). Eighteen of the eyes had grade I papilloedema, whereas grade II, III, and IV papilloedema was found in 26, 12, and eight eyes. No patient of grade V papilloedema was found in the present study population. The same grade of papilloedema in both eyes was found in 18 patients and different grades in both eyes were found in 14 patients. The papilloedema grade did not vary by more than one grade in both eyes and patients who had different papilloedema grades belonged to either grade II or III. The patients were evaluated for anatomical signs of papilloedema on MRI by another independent observer to prevent bias in the observers evaluating the DWI isotropic trace images and ADC maps. ONS enlargement, ON tortuosity, flattening of posterior sclera and intraocular projection of ON papilla were found in 87.5% (56/64), 73.4% (47/64), 57.8% (37/64), and 35.9% (23/64) of the patients, respectively.

The distribution of ONH hyperintensity for cases and control groups and among different grades of papilloedema is shown in Tables 1 and 2, respectively. Highly significant statistical correlation ($p$=0.0001) was found between clinical grade of papilloedema and qualitative grading of ONH hyperintensity on DWI by chi-square test, for both

**Table 1**
Distribution of optic nerve head (ONH) hyperintensity in cases and control groups.

| | Cases ($n$=64) | | | Control participants ($n$=64) | | |
|---|---|---|---|---|---|---|
| | No | Mild | Marked | No | Mild | Marked |
| Observer 1 | 12.5% (8/64) | 54.7% (35/64) | 32.8% (21/64) | 96.8% (62/64) | 3.2% (2/64) | 0% (0/64) |
| Observer 2 | 12.5% (8/64) | 56.3% (36/64) | 31.2% (20/64) | 98.4% (63/64) | 1.6% (1/64) | 0% (0/64) |

**Table 2**
Distribution of optic nerve head (ONH) hyperintensity according to clinical grade.

| Papilloedema grade | Observer 1 | | | Observer 2 | | |
|---|---|---|---|---|---|---|
| | No | Mild | Marked | No | Mild | Marked |
| I ($n$=18) | 44.4% (8/18) | 55.6% (10/18) | 0% (0/18) | 44.4% (8/18) | 55.6% (10/18) | 0% (0/18) |
| II ($n$=26) | 0% (0/26) | 80.8% (21/26) | 19.2% (5/26) | 0% (0/26) | 84.6% (22/26) | 15.4% (4/26) |
| III ($n$=12) | 0% (0/12) | 33.3% (4/12) | 66.7% (8/12) | 0% (0/12) | 33.3% (4/12) | 66.7% (8/12) |
| IV ($n$=8) | 0% (0/8) | 0% (0/8) | 100% (8/8) | 0% (0/8) | 0% (0/8) | 100% (8/8) |

observers. A strong statistical difference ($p$=0.001) was found between the case and control groups for presence of ONH hyperintensity on DWI, by Fisher's exact test, for both observers.

The mean ADC values for each grade of papilloedema and for control patients were calculated and the distribution of the same is shown in Table 3. Both the observers were not able to place ROIs in one ONH in a patient in the case group due to significant image distortion. The normality of distribution of ADC value, calculated by each observer, as well as the mean ADC value was done using the Shapiro–Wilk test, which yielded $p$-values of 0.914, 0.900, and 0.902 for observers 1 and 2 and for mean ADC value, respectively, in case group and $p$-values of 0.535, 0.414, and 0.463, respectively, in control group, suggesting a normal distribution of ADC values of ONH in the case and control groups. A highly significant difference ($p$=0.001) between ADC values of ONH was found between different grades of papilloedema using the ANOVA-F test as well as between cases and control groups by Student's $t$-test for both the observers.

An ROC curve was drawn for ADC values calculated by each observer and mean of ADC values calculated by each observer in case and control participants (Fig 1). A cut-off ADC value was defined for each observer as well as a mean ADC value between two observers to distinguish between case and control groups. The sensitivity, specificity, positive and negative predictive value of ONH hyperintensity on DWI, and the cut-off ADC value to distinguish between cases and controls are shown in Table 4.

The interobserver agreement for qualitative grading of ON head hyperintensity, calculated by kappa statistic, yielded a k-value of 0.975. A Bland–Altman plot (Fig 2), drawn for measurement of interobserver concordance regarding calculation of ADC value of ONH, showed a high concordance between the two observers.

## Discussion

Viets *et al.*[7] first evaluated the presence of ONH hyperintensity in cases of papilloedema and control participants. They found ONH hyperintensity on DWI to be highly specific (100%) as a radiological sign of papilloedema, although it lacked sensitivity (26.3% and 42.1% for two observers). A statistically significant difference between the case and control groups was found in their study. Salvay *et al.*[8] also found significant statistical correlation between papilloedema grades and qualitative grading of ONH hyperintensity. Both the studies were retrospective and the major limitations of these studies stem from the inherent poor resolution of DWI images of the orbit because of

**Table 3**
Distribution of apparent diffusion coefficient (ADC) value of optic nerve head (ONH) in cases (among different grades of papilloedema) and controls.

| | Papilloedema grade | ADC value of ONH ($\times 10^{-6}$ mm$^2$/s) | | | | | |
|---|---|---|---|---|---|---|---|
| | | $N$ | Mean | SD | SE | 95% Confidence interval for mean | |
| | | | | | | Lower bound | Upper bound |
| Observer 1 | Cases | | | | | | |
| | Grade I | 18 | 1729.972 | 155.2815 | 36.6002 | 1652.753 | 1807.192 |
| | Grade II | 25 | 1422.824 | 85.5626 | 17.1125 | 1387.506 | 1458.142 |
| | Grade III | 12 | 1183.275 | 95.8302 | 27.6638 | 1122.387 | 1244.163 |
| | Grade IV | 8 | 963.175 | 117.2423 | 41.4514 | 865.158 | 1061.192 |
| | Total | 63 | 1406.584 | 279.4920 | 35.2127 | 1336.195 | 1476.973 |
| | Controls | | | | | | |
| | Grade 0 | 64 | 1970.863 | 89.9799 | 10.7547 | 1790.040 | 2150.823 |
| Observer 2 | Cases | | | | | | |
| | Grade I | 18 | 1737.661 | 158.6396 | 37.3917 | 1658.771 | 1816.551 |
| | Grade II | 25 | 1423.596 | 84.8203 | 16.9641 | 1388.584 | 1458.608 |
| | Grade III | 12 | 1186.983 | 96.7993 | 27.9435 | 1125.480 | 1248.487 |
| | Grade IV | 8 | 966.088 | 119.9808 | 42.4196 | 865.781 | 1066.394 |
| | Total | 63 | 1410.163 | 281.5502 | 35.4720 | 1339.256 | 1481.071 |
| | Controls | | | | | | |
| | Grade 0 | 64 | 1972.146 | 89.0599 | 10.6447 | 1794.026 | 2150.266 |

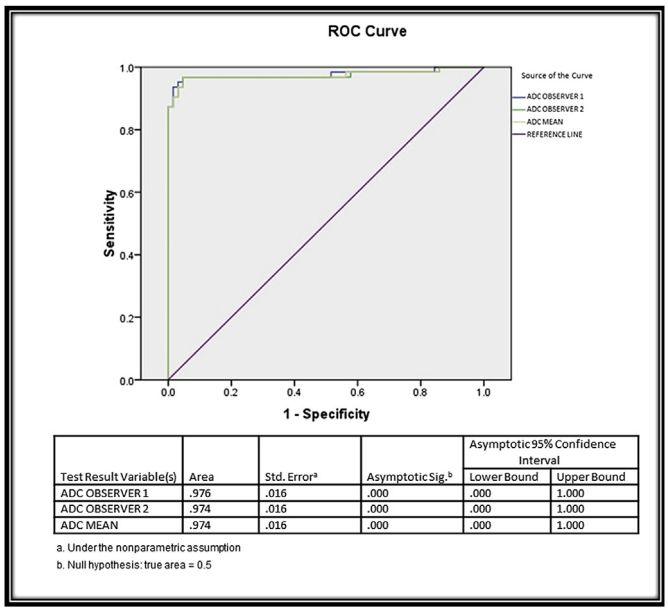


| Test Result Variable(s) | Area | Std. Error[a] | Asymptotic Sig.[b] | Asymptotic 95% Confidence Interval | |
|---|---|---|---|---|---|
| | | | | Lower Bound | Upper Bound |
| ADC OBSERVER 1 | .976 | .016 | .000 | .000 | 1.000 |
| ADC OBSERVER 2 | .974 | .016 | .000 | .000 | 1.000 |
| ADC MEAN | .974 | .016 | .000 | .000 | 1.000 |

a. Under the nonparametric assumption
b. Null hypothesis: true area = 0.5

**Figure 1** The ROC curve for ADC value for both observers and mean ADC value between case and control groups.

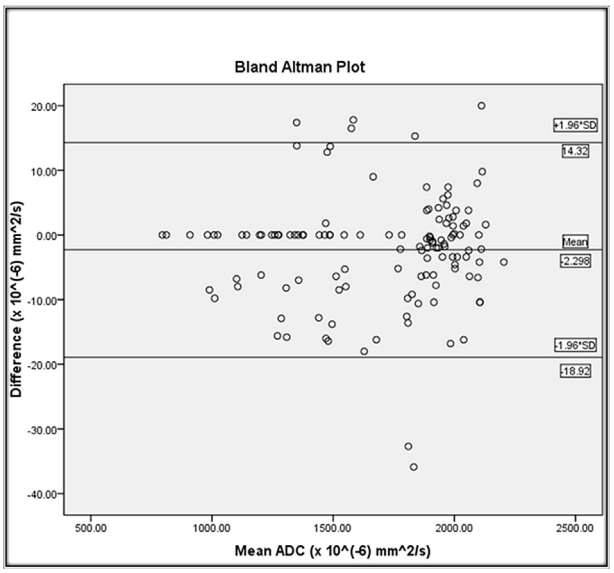


**Figure 2** Bland–Altman analysis for interobserver concordance for ADC value of ONH.

susceptibility artefacts arising from the tissue–bone interface[9] as well as due to partial volume averaging secondary to the higher section gap and section thickness used. Both studies used section thicknesses of 5–7 mm with an intersection gap of 1.5 mm. To the authors' knowledge, the present study was the first prospective study to find a correlation between diffusion parameters of ONH and clinical grades of papilloedema. To overcome the potential drawbacks of conventional orbital DWI, orbital DWI was acquired using dedicated software using DWI-based on readout segmented echo planar imaging and parallel imaging (SYNGO RESOLVE). The ADC values of ONH were also calculated by drawing ROIs on system-generated ADC maps. MRI acquisition was performed on the same day as the clinical examination as raised ICP is a potentially dangerous condition and most of the patients receive treatment on an emergency basis predominantly in the form of drugs lowering ICP. Imaging was done on the same day prior to starting the treatment to obtain maximum clinicoradiological correlation. Being a manifestation of raised ICP, papilloedema is generally symmetrical bilaterally; however, in the present study each ONH was studied separately as the papilloedema grades in both eyes were different in 14 patients, which varied maximally by one integer grade. This was done to reflect the relationship between the diffusion parameters of ONH and clinical grade of papilloedema.

The results of the present study indicate that the presence of ONH hyperintensity in papilloedema cases can serve as a potential imaging sign of papilloedema and thereby raised ICP. Moreover, highly significant statistical correlation was found between qualitative grading of ONH hyperintensity and clinical grade of papilloedema. Significant statistical differences were also found between cases and controls for the presence of ONH hyperintensity. The criteria proposed by Viets *et al.*[7] was used for grading ONH hyperintensity. In addition, the ADC values of ONH hyperintensity was also found to be statistically significant among different grades of papilloedema and there is a decreasing trend of ADC value with increasing clinical grade of papilloedema (Figs 3–5, Table 3). The difference in ADC values of ONH between cases and controls was also statistically significant and the mean cut-off ADC value to distinguish between the cases and controls was obtained. Thus, it can be concluded that clinical grading of papilloedema bears a statistically significant relationship with ONH hyperintensity on DWI and the ADC value of ONH.

A few implications can be drawn from the present study. Most importantly, ONH hyperintensity can be a useful imaging sign of papilloedema. Although the statistical significance of its presence or absence was not compared with the presence or absence of other anatomical signs of raised ICP on MRI, it may be possible that ONH hyperintensity can be found in patients with papilloedema when other signs

**Table 4**
Sensitivity, specificity, positive and negative predictive value of optic nerve head (ONH) hyperintensity and apparent diffusion coefficient (ADC) cut-off value to distinguish between cases and controls.

| Diffusion parameter of ONH | Sensitivity | Specificity | Positive predictive value | Negative predictive value |
|---|---|---|---|---|
| ONH hyperintensity | | | | |
| Observer 1 | 87.5% | 97.1% | 96.6% | 89.5% |
| Observer 2 | 87.5% | 98.6% | 98.2% | 89.6% |
| Cut-off ADC value | | | | |
| Observer 1 ($1802.31\times10^{-6}$ mm$^2$/s) | 93.65% | 98.44% | 98.33% | 94.03% |
| Observer 2 ($1853.45\times10^{-6}$ mm$^2$/s) | 96.83% | 95.31% | 95.31% | 96.82% |
| Mean ADC ($1844.52\times10^{-6}$ mm$^2$/s) | 96.83% | 95.31% | 95.31% | 96.82% |

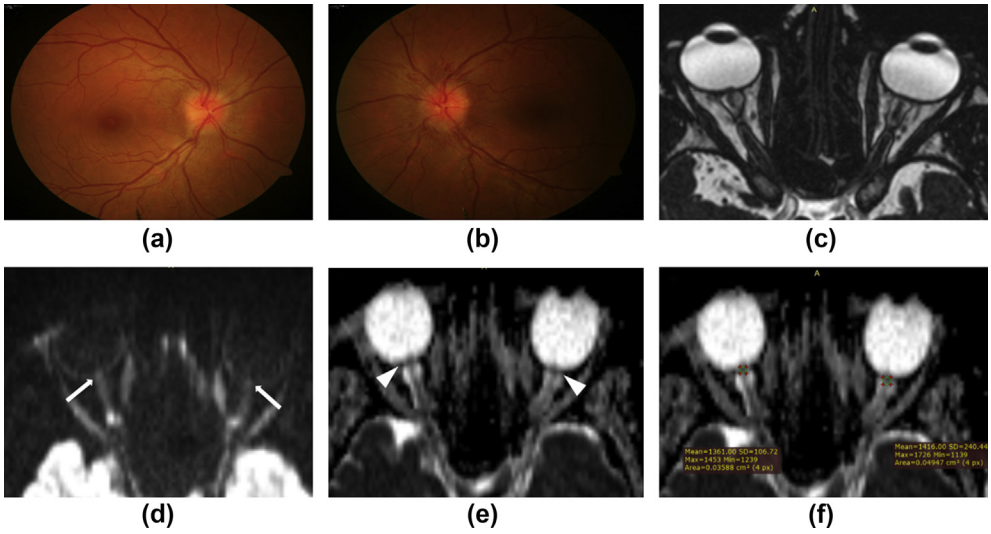


**Figure 3** Colour fundus photographs of (a) right and (b) left eyes of a 29-year-old female patient who had grade II papilloedema bilaterally. (c) Axial CISS sequence at the level of the orbit shows the presence of tortuous bilateral ONs with bilateral ONS enlargement and posterior scleral flattening and intraocular protrusion of right ONH. (d) Axial DWI isotropic trace images (b=1,000) for bilateral ONs and the corresponding ADC map (e) for bilateral ONs. DWI isotropic trace images show mild hyperintensity at bilateral ONH (shown by arrows). ADC maps show hypointensity at the area corresponding to the area of hyperintensity at bilateral ONH respectively (shown by arrowheads). (f) ROIs placed at the right and left ONH on the ADC map at the region of hypointensity and the ADC values obtained are shown in the images (right ONH: $1361\times10^{-6}$ mm$^2$/s, left ONH: $1416\times10^{-6}$ mm$^2$/s).

are absent, which was the case with two of the present patients (Fig 5). Although, the previous studies by Viets *et al.*[7] and Salvay *et al.*[8] reported a lower sensitivity and high specificity of this sign, the present study found this sign to be highly sensitive as well as specific and having high positive and negative predictive values (Table 4). It suggests that the likelihood of false-negative or false-positive ONH hyperintensity in the setting of papilloedema is extremely

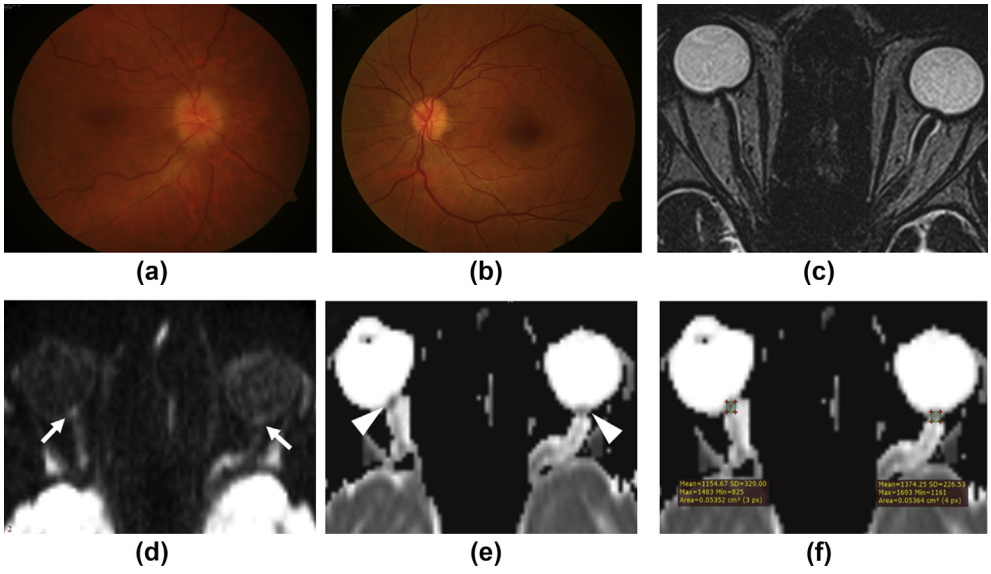


**Figure 4** Colour fundus photographs of (a) right and (b) left eyes of a 36-year-old female patient with grade III papilloedema (nasal and temporal disc margin blurring with obscuration of the vessels at periphery but not at the centre) right and grade II papilloedema (obliteration of optic cup with blurring of disc margin on both nasal and temporal side without vessel obscuration) left. (c) Axial CISS sequence at the level of the orbit shows the presence of tortuous bilateral ONs with bilateral ONS enlargement and posterior scleral flattening and intraocular protrusion of bilateral ONH. (d) Axial DWI isotropic trace images (b=1,000) and (e) corresponding ADC maps for bilateral ON, respectively. DWI isotropic trace images show marked hyperintensity at the right ONH and mild hyperintensity at the left ONH (shown by arrows). ADC maps show hypointensity at the area corresponding to the area of hyperintensity at bilateral ONHs (shown by arrowheads). (f) ROI placed at the right and left ONH on the ADC map at the region of hypointensity and the ADC values obtained are shown in the images (right ONH: $1154.67\times10^{-6}$ mm$^2$/s, left ONH: $1374.25\times10^{-6}$ mm$^2$/s).

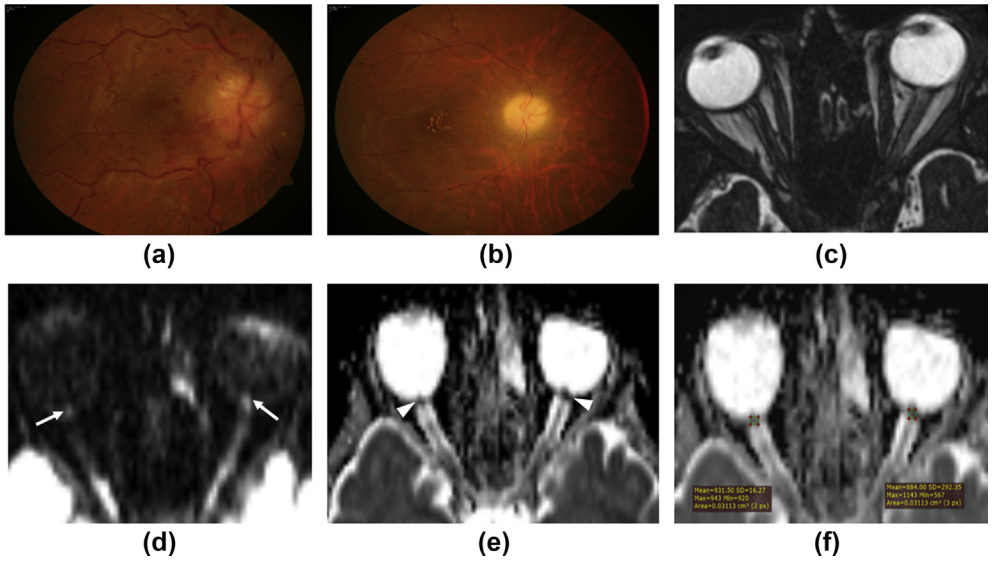


**Figure 5** Colour fundus photographs of (a) right and (b) left eyes of a 23-year-old female patient with grade IV papilloedema (blurring of disc margin on nasal and temporal aspect with obscuration of vessels at disc margin as well as at the centre and pale disc on left) in both. (c) Axial CISS sequence at the level of the orbit does not show the presence of any anatomical signs of papilloedema. (d) Axial DWI isotropic trace images (b=1,000) and (e) corresponding ADC maps for the bilateral ONs. DWI isotropic trace images show marked hyperintensity at the bilateral ONHs (shown by arrows). ADC maps show hypointensity at the area corresponding to the area of hyperintensity at the bilateral ONHs (shown by arrowheads). (f) ROI placed at the right and left ONHs on the ADC map at the region of hypointensity and the ADC values obtained are shown in the images (right ONH: $931.5\times10^{-6}$ $mm^2/s$, left ONH: $884\times10^{-6}$ $mm^2/s$).

low. Hence, the presence of ONH hyperintensity on DWI isotropic trace images should alert the radiologist to the possibility of raised ICP and may warrant a communication with the clinician for further evaluation of the patient.

Moreover, the ADC value of ONH has shown a gradually declining trend with increasing clinical grades of papilloedema suggesting that the degree of true diffusion restriction increases with increasing clinical grade. Indeed, the ADC value of ONH can be used as an indirect quantitative measure of raised ICP in appropriate clinical settings. In addition, a mean cut-off ADC value of ONH ($1844.52\times10^{-6}$ $mm^2/s$) was defined in the present study, which could help distinguish between cases and controls with high sensitivity, specificity and positive and negative predictive values (Table 4); however, the relatively high PPV needs to be interpreted with caution, because in the general population, the prevalence of papilloedema is much lower than that in the present study (50%). Although in the present study follow-up imaging was not performed, the ADC value of ONH can be expected to be a useful parameter for treatment monitoring and follow-up of patients with papilloedema. With response to treatment or improvement, an increasing trend of the ADC value can be expected. Furthermore, it might be possible that radiological grading of papilloedema can be proposed based on the ADC values of ONH; however, this would require a larger sample size.

Finally, rs-EPI-based DWI was used rather than routine ss-EPI-based DWI to reduce the susceptibility and blurring artefacts associated with the conventional DWI to improve image quality.[9] Calculation of the ADC value of ONH is a challenging task owing to the smaller size of ONH as well as due to presence of susceptibility and blurring artefacts at tissue interfaces. As previous studies have shown that rs-EPI-based DWI can improve image quality in challenging body regions such as the orbit, this technique was chosen over conventional DWI to obtain better quality images and optimum placement of the ROIs on ADC maps. In addition, for better visualisation of ONH the section thickness was reduced to 2 mm for acquiring DWI images, which was higher (5–7 mm) in the previous studies.[7,8] This may be the reason for obtaining significantly higher sensitivity at DWI compared to the previous studies[7,8]; however, because of the small area of ONH, the possibility of partial volume averaging still exists even with a section thickness of 2mm and intersection gap of 0.4 mm. On reducing the section thickness further, however, the images obtained were too noisy to interpret and it would have increased the acquisition time significantly. In the present study, the acquisition time for DWI is high compared to ss-EPI-based diffusion. Further reduction of duration with rs-EPI-based diffusion can be achieved by simultaneous multisection acceleration using blipped-CAIPI (controlled aliasing in parallel imaging) modifications.[19] The MRI sequences in the present study were acquired using a 1.5 T system, but using a 3 T or higher strength could further improve the images using the same technique.[19] Another reason that might be a factor in having an increased sensitivity of the ONH hyperintensity on DWI in the present study could be the acquisition of MRI on the same day as the clinical examination.

The present study has many potential limitations. As no follow-up imaging was obtained for the patients, the temporal sequence of change in diffusion parameters in different stages of papilloedema could not be assessed, which would have possibly elucidated the pathogenesis of

papilloedema; however, as papilloedema, especially in the setting of IIH, runs a chronic course, the follow-up imaging requires a longer duration than afforded by the study period.

Furthermore, the diffusion parameters of ONH were not compared with other visual parameters such as visual acuity and visual field mean diameter. This is because optic atrophy secondary to chronically raised ICP takes years to set in and often visual parameters other than the clinical grade of papilloedema are normal or mildly abnormal in a significant number of patients. Thus, comparison with the other visual parameters would have required a long-term follow-up.

The correlation of the diffusion parameters with ONH with CSF opening pressure was also not done in the present patient cohort. CSF opening pressure was measured in the setting of raised ICP only after ruling out possible intracranial space-occupying lesions by cross-sectional studies to prevent possible cerebellar coning. As the MRI was undertaken in the patient group on the same day as the clinical evaluation, it served the need for cross-sectional imaging. The patients were started on medical treatment to lower ICP immediately after MRI. The CSF opening pressure was calculated in the subset of patients diagnosed with IIH or meningitis, after a mean time interval of 1–3 days of MRI acquisition. As this can directly reflect the ICP, a correlation between diffusion parameters of ONH and the CSF opening pressure would have rendered the present study with more relevance; however, as these patients have already received treatment for lowering the ICP, the maximum correlation CSF opening pressure with diffusion parameters of ONH was difficult to establish in these clinical settings.

Finally, it can be argued that placement of ROIs at the ONH for calculating ADC values can be error prone due to the small size of the ONH as well as the presence of surrounding CSF spaces and vitreous humour. In the present study, a stringent protocol was followed for placing the ROI at the ONH (as shown in Figs 3f, 4f, 5f). Strong interobserver concordance (Fig 2) was found in the present study regarding calculation of ADC value of ONH. Hence, it can be concluded the ADC value of the ONH can be calculated with good accuracy by following a strict protocol.

To the authors' knowledge, the present study is the first prospective study to evaluate the presence of ONH hyperintensity in patients with papilloedema and calculate the ADC values of the ONH. It can be opined that the presence of ONH hyperintensity in papilloedema patients is because of true diffusion restriction and supports the ischaemic theory of the pathogenesis of papilloedema. As papilloedema runs an indolent course with minimal visual symptoms, specially in cases of IIH, it is important to diagnose it as early as possible to prevent optic atrophy and visual impairment. On the other hand, papilloedema is a manifestation of raised ICP, which requires urgent treatment. Thus, it is important for radiologists to identify ONH hyperintensity on DWI, as well as the lower ADC values of ONH, and alert the clinician about the likely presence of raised ICP. The anatomical signs of papilloedema on imaging have variable sensitivity and specificity, and it could be possible that the presence of true diffusion restriction at the ONH can be established in future as a definite sign of papilloedema and its presence can provide the clue to the diagnosis of raised ICP in appropriate clinical settings.

In conclusion, the presence of ONH hyperintensity on DWI is a potential imaging marker of papilloedema and qualitative grading of ONH hyperintensity as well as ADC values of ONH correlates well with the clinical grade of papilloedema. Diffusion parameters of ONH can be used in future as an indirect measure of ICP in appropriate clinical settings.

## Conflict of interest

The authors declare no conflict of interest.

## References


1. Whiting AS, Johnson LN. Papilledema: clinical clues and differential diagnosis. *Am Fam Physician* 1992;**45**(3):1125–34.
2. Passi N, Degnan AJ, Levy LM. MR imaging of papilledema and visual pathways: effects of increased intracranial pressure and pathophysiologic mechanisms. *AJNR Am J Neuroradiol* 2013;**34**(5):919–24. https://doi.org/10.3174/ajnr.A3022.
3. Seitz J, Held P, Strotzer M, *et al*. Magnetic resonance imaging in patients diagnosed with papilloedema: a comparison of 6 different high-resolution T1- and T2(*)-weighted 3-dimensional and 2-dimensional sequences. *J Neuroimaging* 2002;**12**(2):164–71.
4. Padhye LV, Van Stavern GP, Sharma A, *et al*. Association between visual parameters and neuroimaging features of idiopathic intracranial hypertension. *J Neurol Sci* 2013;**332**(1–2):80–5. https://doi.org/10.1016/j.jns.2013.06.022.
5. Turner R, Le Bihan D, Chesnick AS. Echo-planar imaging of diffusion and perfusion. *Magn Reson Med* 1991;**19**(2):247–53.
6. Hagmann P, Jonasson L, Maeder P, *et al*. Understanding diffusion MR imaging techniques: from scalar diffusion-weighted imaging to diffusion tensor imaging and beyond. *RadioGraphics* 2006;**26**:S205–23. https://doi.org/10.1148/rg.26si065510.
7. Viets R, Parsons M, Van Stavern G, *et al*. Hyperintense optic nerve heads on diffusion-weighted imaging: a potential imaging sign of papilledema. *AJNR Am J Neuroradiol* 2013;**34**(7):1438–42. https://doi.org/10.3174/ajnr.A3388.
8. Salvay DM, Padhye LV, Huecker JB, *et al*. Correlation between papilledema grade and diffusion-weighted magnetic resonance imaging in idiopathic intracranial hypertension. *J Neuroophthalmol* 2014;**34**(4):331–5. https://doi.org/10.1097/WNO.0000000000000150.
9. Kapur R, Sepahdari AR, Mafee MF, *et al*. MR imaging of orbital inflammatory syndrome, orbital cellulitis, and orbital lymphoid lesions: the role of diffusion-weighted imaging. *AJNR Am J Neuroradiol* 2009;**30**(1):64–70. https://doi.org/10.3174/ajnr.A1315.
10. Porter DA, Heidemann RM. High resolution diffusion-weighted imaging using readout-segmented echo-planar imaging, parallel imaging and a two-dimensional navigator-based reacquisition. *Magn Reson Med* 2009;**62**(2):468–75. https://doi.org/10.1002/mrm.22024.
11. Morelli J, Porter D, Ai F, *et al*. Clinical evaluation of single-shot and readout-segmented diffusion-weighted imaging in stroke patients at 3 T. *Acta Radiol* 2013;**54**(3):299–306. https://doi.org/10.1258/ar.2012.120541.
12. Yeom KW, Holdsworth SJ, Van AT, *et al*. Comparison of readout-segmented echo-planar imaging (EPI) and single-shot EPI in clinical application of diffusion-weighted imaging of the pediatric brain. *AJR Am J Roentgenol* 2013;**200**(5):W437–43. https://doi.org/10.2214/AJR.12.9854.
13. Wei XE, Li WB, Li MH, *et al*. Detection of brain lesions at the skull base using diffusion-weighted imaging with readout-segmented echo-planar imaging and generalized autocalibrating partially parallel acquisitions. *Neurol India* 2011;**59**(6):839–43. https://doi.org/10.4103/0028-3886.91361.

14. Zhao M, Liu Z, Sha Y, *et al*. Readout-segmented echo-planar imaging in the evaluation of sinonasal lesions: a comprehensive comparison of image quality in single-shot echo-planar imaging. *Magn Reson Imaging* 2016;**34**(2):166–72. https://doi.org/10.1016/j.mri.2015.10.010.
15. Xu XQ, Liu J, Hu H, *et al*. Improve the image quality of orbital 3 T diffusion-weighted magnetic resonance imaging with readout-segmented echo-planar imaging. *Clin Imaging* 2016;**40**(4):793–6.
16. Wan H, Sha Y, Zhang F, *et al*. Diffusion weighted imaging using readout-segmented echo-planar imaging, parallel imaging, and two-dimensional navigator-based reacquisition in detecting acute optic neuritis. *J Magn Reson Imaging* 2016;**43**:655–60. https://doi.org/10.1016/j.clinimag.2016.03.002.
17. Frisén L. Swelling of the optic nerve head: a staging scheme. *J Neurol Neurosurg Psychiatry* 1982;**45**(1):13–8.
18. Scott CJ, Kardon RH, Lee AG, *et al*. Diagnosis and grading of papilloedema in patients with raised intracranial pressure using optical coherence tomography vs clinical expert assessment using a clinical staging scale. *Arch Ophthalmol* 2010;**128**(6):705–11. https://doi.org/10.1001/archophthalmol.2010.94.
19. Frost R, Jezzard P, Douaud G, *et al*. Scan time reduction for readout-segmented EPI using simultaneous multislice acceleration: diffusion-weighted imaging at 3 and 7 Tesla. *Magn Reason Med* 2015 Jul;**74**(1):136–49. https://doi.org/10.1002/mrm.25391.